J. Coat. Technol. Res., **19** (4) 1055–1066, 2022
https://doi.org/10.1007/s11998-021-00584-9

Preparation and characterization of cationic waterborne polyurethanes containing a star-branched polydimethylsiloxane

Xiaoling He, Jingwei He, Yangkun Sun, Xiaopei Zhou, Jingying Zhang, Fang Liu

Received: 10 September 2021 / Revised: 2 November 2021 / Accepted: 14 November 2021

Abstract Cationic waterborne polyurethanes (CWPUs) bring in hydrophilic component to molecular chain, which inevitably deteriorates its water-resistant ability. Here, we synthesized a series of branched chain cationic waterborne polyurethanes (i.e., CWPUs-Si) that had been modified using a novel star-branched polydimethylsiloxane (SB-PDMS) to improve their water-resistant performance. The effects of SB-PDMS content on the properties of the CWPUs-Si polymers (e.g., crystallinity, emulsion stability, mechanical performance, surface element enrichment, surface topography, water resistance), together with the performance of coatings prepared by cathodic electrodeposition, were determined. The results showed that the introduction of SB-PDMS increased phase separation and surface roughness induced by hydrogen bonding while the surface energy decreased, both of which improved water resistance. The polymers showed improved rigidity due to increased content of the hard segments and enhanced physical crosslinking. Except for an increase in pencil hardness, SB-PDMS had no effect on the films prepared by cathodic electrodeposition. The results from this study may provide a strategy to improve the water-resistant properties of CWPUs.

X. He, J. He, Y. Sun, X. Zhou, F. Liu (✉)
School of Materials Science and Engineering, South China University of Technology, Guangzhou 510640, Guangdong, China
e-mail: mcfliu@126.com

X. He, J. Zhang (✉)
Key Laboratory of 3D Printing Technology in Stomatology, The First Dongguan Affiliated Hospital, Guangdong Medical University, Dongguan 523710, Guangdong, China
e-mail: zhangjy@gdmu.edu.cn

Keywords Cationic waterborne polyurethane, Cathodic electrodeposition coatings, Star-branched polydimethylsiloxane, Water-resistant ability

Introduction

Waterborne polyurethanes (WPUs) are novel functional polymers widely used as adhesives and coatings, particularly for textiles such as leather, due to their desirable physicochemical properties.[1–7] However, the formation of emulsions resulting from the use of aqueous processing dispersants in the presence of internal hydrophilic cationic groups, inevitably compromises the water-resistant performance of the WPUs coatings. Common approaches to resolve this issue include the introduction of crosslinked network structures, or low surface energy units, via chemical modification or physical blending.[8–14]

Chemical modifications, such as thermal curing crosslinking and radiation crosslinking, can enhance the water resistance and mechanical strength of WPUs by forming intersecting network structures.[15–18] Nonetheless, the formation of crosslinked network structures has scarcely any improvement for the water contact angle of WPU which limits its application area of requiring a hydrophobic surface. Although physical blending of WPUs with hydrophobic nano-materials, e.g., SiO_2, TiO_2, halloysite nanotubes and graphene oxide, can also improve the water resistance,[19–22] aggregation in the WPU matrix can impair sustained emulsion stability and subsequent performance of the polymer. However, recent studies have shown that limitations associated with small water contact angles and agglomeration could be overcome by the introduction of low surface energy units into WPU (by chemical modification).[23,24]

Polydimethylsiloxane (PDMS) is a non-toxic, thermally stable, low surface energy organic silicone, while

its chemistry is readily amenable to introduction into the backbone or side chains of WPU. Zheng et al.[25] and Sharma et al.[26] showed that WPU prepared with functional PDMS polyether in the backbone had significantly improved hydrophobic properties due to the outward migration of low surface energy units. The introduction of PDMS also increased the water resistance of prepared coatings by increasing the degree of micro-phase separation.[27]

In general, the hydrophobic modification of WPUs using organosilicon chemistry requires surface enrichment with siloxane groups and increased surface roughness for improved water resistance.[28] In particular, the migration of hydrophobic siloxane groups to the surface of the WPU film forms a silicone-rich nanoscale layer which significantly increases the water contact angle of the polymer.[29,30] Although the migration of siloxane groups may exhibit thermodynamic behavior, their location is also important. Normally, the migration of siloxane groups increases with increasing temperature due to the associated increase in segment motion of the polymer. In siloxane-modified WPUs, the groups can be inserted into the backbone or the side chain. Siloxane groups on the backbone must overcome greater resistance to migrate the surface of WPUs film compared with those in the side chain. Consequently, the introduction of siloxane groups into the side chain of WPU may be the preferred strategy for optimum performance.

Cathodic electrodeposition (CED) is an industrial process widely used to apply coatings, e.g., to fabricated metal components. An essential requirement of CED is the maintenance of a positive charge on the (WPUs) coating particles. Under an applied external electric field, the positively charged particles can then migrate and deposit on the cathodic electrode to form a uniform film.

Here, we prepared a series of cationic WPUs (CWPUs) modified by the introduction of a novel star-branched (SB)PDMS side chain, i.e., CWPUs-Si. SB-PDMS possess three long and separate PDMS chains, which facilitates the formation of a silicone-rich nanoscale layer compared with polymers incorporating single PDMS chains. The effects of SB-PDMS content on the properties of the prepared CWPUs-Si emulsions and films were thoroughly investigated and the results discussed in detail. The results from this investigation may provide a basis to enhance the hydrophobicity of CWPUs coatings by decreasing their surface energy and constructing micro-nano-surface structures.

Experimental

Materials

Isophorone diisocyanate (IPDI) was supplied by BASF Aktiengesell Ltd. 1,4-Butanediol (BDO) and di-n-butyltin dilaurate (DBTDL) were purchased from Tokyo Chemical Industry Ltd. N-Methyldiethanolamine (N-MDEA) was supplied by Acros Organics. Polycaprolactone diol (PCL, Mn=1000 g/mol) was obtained from Daicel Chemical Industries Ltd. SB-PDMS was obtained from Maitu Silicone Co., Ltd, China. PCL was desiccated under vacuum at 80°C for 24 h before use. BDO, N-MDEA, and acetone were dried over 4 Å molecular sieves for at least one week before use. Other chemicals and solvents were applied as obtained without any additional purification.

Synthesis of CWPUs-Si

The PCL, IPDI, and DBTDL were put into a 250-mL three-necked round bottom flask equipped with a mechanical stirrer, thermometer, and condenser. The relative composition is shown in Table 1. First, the reaction was performed in an oil bath at 40°C for 0.5 h and then at 80°C until the NCO content reached a theoretical value monitored by dibutylamine back titration method. Subsequently, the BDO was added into flask and the reaction mixture proceeded at 80°C for 2.5 h. After that, the reaction mixture was cooled down to 40°C, the N-MDEA dissolved in acetone was added dropwise for 0.5 h, and then, the reaction mixture was heated to 70°C and the prepolymer continued to extend chain for 2 h. A few drops of ethanol were added to ensure a complete reaction of the isocyanate.

An appropriate amount of acetone was added to reduce the viscosity of reaction mixture when the viscosity became too high. Then, the SB-PDMS was added into the flask and the reaction proceeded at 80°C for 2.5 h. Afterward, the reaction mixture was cooled down to 40°C, and acetic acid (HAc) dissolved in acetone was added dropwise to neutralize the tertiary amine group for 2 h. Finally, the deionized water was added dropwise into the flask under vigorous stirring. The CWPUs-Si with solid content of 30 wt% were obtained after removing the acetone with a rotary evaporator.

During the synthesis of CWPUs-Si, the molar ratio of NCO to OH and the neutralization degree were kept at 1. 1 and 80%, respectively. A series of CWPUs containing SB-PDMS weight percentage of 1% (CWPUs-Si1), 3% (CWPUs-Si3), 5% (CWPUs-Si5), 7% (CWPUs-Si7), 9% (CWPUs-Si9), and 11% (CWPUs-Si11) were prepared. For comparison, the CWPUs without SB-PDMS (CWPUs-Si0) were also synthesized by using the same protocol. The chemical compositions of synthesized CWPUs-Si are summarized in Table 1.

Preparation of CWPUs-Si cast films and CED coatings

The cast films were prepared by pouring CWPUs-Si emulsion (weight: 30 g; solid content: 30 wt%) into

Table 1: The composition design of CWPUs-Si

Sample	[a]R	Composition (mmol)						[b]N-MDEA (wt%)	[c]SB-PDMS (wt%)	Hard segment content (wt%)
		IPDI	PCL	N-MDEA	BDO	HAc	SB-PDMS			
CWPUs-Si0	1.2	150	58.2	66.8	11.4	53.4	0	8	0	43.9
CWPUs-Si1	1.3	150	52.6	62.7	20.6	50.2	0.39	8	1	47.0
CWPUs-Si3	1.4	150	47.9	59.3	28.1	47.4	1.12	8	3	50.4
CWPUs-Si5	1.5	150	43.7	56.3	34.5	45.0	1.83	8	5	53.5
CWPUs-Si7	1.6	150	40.1	53.6	40.1	42.9	2.51	8	7	56.5
CWPUs-Si9	1.7	150	37.0	51.3	45.0	41.0	3.18	8	9	59.3
CWPUs-Si11	1.8	150	34.1	49.2	49.2	39.4	3.84	8	11	62.0

[a]R=n(IPDI)/[n(PCL)+n(N-MDEA)]; [b]The weight percent of N-MDEA is based on the prepolymer; [c]The weight percent of SB-PDMS is based on the total weight of the prepolymer.

teflon disk (100 mm×100 mm × 10 mm) and desiccated under ambient conditions for 7 days. The final CWPUs-Si films were obtained after being heated at 60°C in vacuum oven for 24 h.

The CWPUs-Si emulsion with 30 wt% of solid content was diluted with deionized water to 10 wt. % of solid content at an agitation speed of 500 rpm to prepare CED coatings. The CED process was carried out on tinplate with the dimensions of 50 mm × 120 mm × 0.28 mm at 25°C for 120 s using 35 V direct current voltage, and the distance from anode to cathode was 50 mm. Then, the well-stirred CWPUs-Si were deposited on the surface of tinplate (cathode) under electric field. After that, the coated stainless steels were first dried at 80°C for 10 min and then at 130°C for 0.5 h and stored in a desiccator for 24 h before testing.

Characterization

Chemical structures of cationic WPUs were characterized on a Thermo Scientific Nicolet iS50 Fourier transform infrared (FTIR) spectrometer using the attenuated total reflectance (ATR) model. The spectra were scanned 32 times within the range of 400–4000 cm^{-1} at a resolution of 8 cm^{-1}.

Dynamic light scattering (DLS) measurements were performed using HORIBA Nano Particle Analyzer SZ-100 to determine the particle size (in Z-average size) and distribution of diluent CWPUs emulsion after an ultrasonic treatment for 5 min. Viscosity of CWPUs-Si emulsion was measured at 25°C by a Brookfield DV-II Pro EXTRA rotational viscometer using the No.4 rotor with a speed of 200 rpm. The stability of CWPUs-Si emulsion was characterized by centrifugal settling method according to GB/T 6753.3-1986. The emulsions were kept in Xiangyi TG16-WS super centrifuge at the speed of 3000 r/min for 15 min by using No.7 rotor, and the centrifugation sediment was recorded as the qualitative evaluation index of emulsion stability.

Surface element analysis of CWPUs-Si film was conducted by the X-ray photoelectron spectroscopy analyzer (XPS, Thermo Fisher ESCALAB XI+) equipped with a single Al Kα X-ray source (1486.6eV, 6 mA×15 kV).

The surface morphology of CWPUs-Si film was observed by Zeiss Merlin field emission scanning electron microscope (SEM) with the accelerating voltage of 5.0 kV.

The crystallization of CWPUs-Si film was researched by X-ray diffractometer (XRD, X' Pert3 Power) with 2θ ranging from 5 to 70° at a speed of 0.2 s/step using scanning step length of 0.02°.

Static contact angle of deionized water or diiodomethane at the air−film interface was measured with a Contact Angle System OCA40 (Dataphysics) at room temperature, where a sessile drop of 3 μL of liquid was used. The data recorded were calculated by the average value of five different locations on one sample. Surface free energy of CWPUs-Si film was determined by the following equations (1) and (2) using the Owens−Wendt−Rabel−Kaelble method.[31]

$$\gamma_s = \gamma_s^d + \gamma_s^p \quad (1)$$

$$\gamma_L(1+\cos\theta_L) = 2\left(\gamma_L^d+\gamma_s^d\right)^{1/2} + 2\left(\gamma_L^P+\gamma_s^P\right)^{1/2} \quad (2)$$

where γ_s is the surface free energy of solid film, γ_s^d is the dispersive components, and γ_s^p is polar component. The testing liquids used were water and diiodomethane, and their γ_L, γ_L^d, and γ_L^P were known values that can be obtained from the relevant criteria.[32]

Tailored film samples (20 mm×20 mm) were immersed in deionized water at 25°C to measure the water absorption calculated by the following equation (3):

$$\text{Water absorption}(\%) = \frac{W_t - W_0}{W_0} \times 100\% \quad (3)$$

where W_o is the weight of the dried sample, and W_t is the weight of sample after water immersion of 24 h.

The tensile test of CWPUs-Si film with dumbbell shape (28 mm in length, 4 mm in width, and 0.8 mm in thickness) was conducted on UT-2080 universal testing machine at a rate of 500 mm/min. The data of each sample were averaged from three specimens.

The dynamic thermo-mechanical property of CWPUs-Si strips (40 mm in length, 6 mm in width, and 0.8 mm in thickness) were investigated on a dynamic mechanical analyzer (DMA TA Q800) at tensile mode using the angular frequency of 1 Hz and amplitude of 10 μm. The scanning temperature ranged from −80°C to 80°C at a heating rate of 3°C/min.

Pencil hardness was measured with a PPH-1 pencil scratch hardness tester according to ISO standard 15184:1998. Cross-cut test was used to measure the adhesion of CED film to stainless steel according to ISO standard 2409:1992. Physical bending test was performed for evaluating flexibility of CWPUs-Si films according to ISO standard 1519:2002. Impact resistance was conducted according to ISO standard 6272-1:2002, and the weight of drop hammer was 1000 g.

Results and discussion

Synthesis and characterization of CWPUs-Si

Hydrophobic SB-PDMS units were grafted into the side chain of CWPUs to enhance the water-resistant performance of the prepared coatings. The polymers were prepared according to the synthetic route given in Scheme 1.

ATR-FTIR was used to verify the incorporation of SB-PDMS into the CWPUs at each addition level (Fig. 1).

The FTIR spectra obtained from each sample showed absorption peaks typical of polyurethane at 3336 cm^{-1} [ν(N-H)], 1716 cm^{-1} [ν(C=O)], 1521 cm^{-1} [δ(N-H)], 1239 cm^{-1} [ν(C-O-C)], and 1033 cm^{-1} [ν(C-N), tertiary amine]. Absorption peaks characteristic of SB-PDMS could be observed in the spectra of CWPUs-Si. Peaks at 1258 cm^{-1}, 801 cm^{-1}, and 1025 cm^{-1} corresponded to the symmetric bending of Si-CH3, rocking of Si-CH3 and asymmetric stretching vibrations of Si-O-Si, respectively. The absorption peaks of Si-O-Si (1025 cm^{-1}) overlapped with those of C-N (1033 cm^{-1}). As the content of SB-PDMS increased in each polymer, the intensity of the silicon absorption peaks also increased, especially those at 1025 cm^{-1} and 801 cm^{-1}. At the same time, the carbonyl absorption peaks shifted from 1716 cm^{-1} (CWPUs-Si0) to 1700 cm^{-1} (CWPUs-Si11), which could be attributed to increased carbonyl hydrogen bonding as the incorporation of SB-PDMS increased.

Emulsion properties of the CWPUs-Si polymers

Emulsion properties can have a large influence on the processability and storage stability of each CWPUs polymer; hence, the effects of SB-PDMS addition on the particle size, viscosity, pH, and centrifugation sediment of the polymer emulsions were studied (Fig. 2 and Table 2).

The Z-average particle size of each CWPUs-Si increased (from 73.6 nm to 374.1 nm) with increasing SB-PDMS content (from 0 to 11 wt%; Table 2), which could be attributed to the simultaneous increase in hydrophobic-branched SB-PDMS groups within the polymer. Conversely, the viscosity of each CWPUs-Si decreased [from 680 mPa·s (CWPUs-Si0) to 16 mPa·s (CWPUs-Si11)] with incremental SB-PDMS addition as the increasing hydrophobicity of the polymers diminished the cohesive forces between the emulsion particles and the water.

Except for CWPUs-Si11, all emulsions exhibited good centrifugal stability with no sedimentation. Presumably, at the highest addition level, excessive branching of SB-PDMS groups may result in surface exposure. Under this condition, the emulsion particles are no longer stabilized by the hydrophilic protonated tertiary amine cation, resulting in some demulsification.[33,34] As the addition of SB-PDMS increased, the emulsion became increasingly turbid (Fig. 2b), changing from a translucent, milky white with a blue tint, to a strong milky white. These observations may stem from enhanced light scattering as the size of the emulsion particles increased.[33,34]

Surface element analysis of CWPUs-Si

Since migration of the low surface energy units to the polymer/air interface was believed to be a thermodynamics process, observation of surface enrichment was deemed possible, even for polymers with very few low surface energy units. To study this phenomenon, XPS equipped with an ion beam etching system was used to determine the elemental composition of each CWPUs-Si at different depths. The detection depth was 10.8 nm for samples without etching. This increased to 12.6 and 14.4 nm for samples etched for 30 and 60 s (etching rate, 0.06 nm/s).

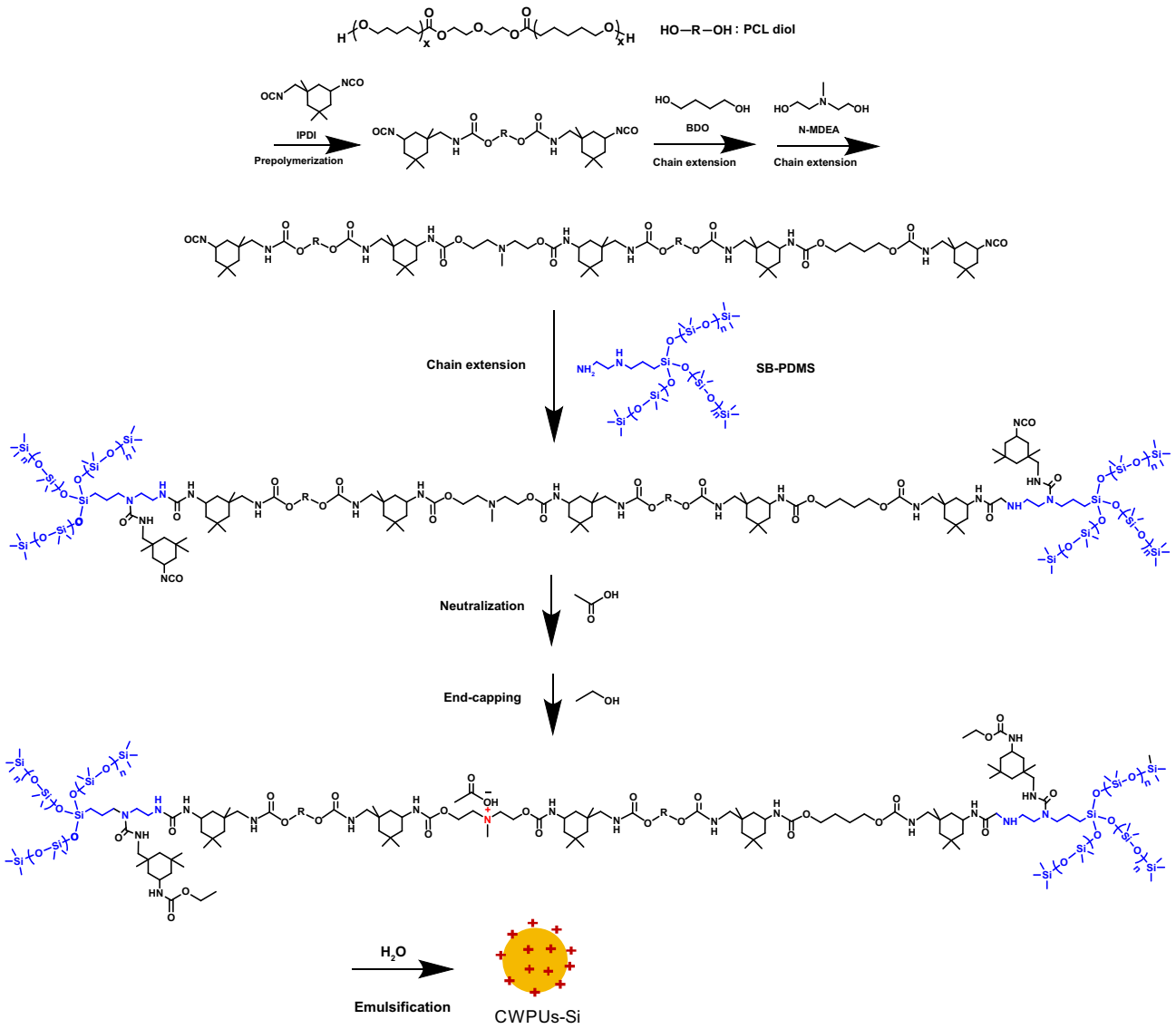

Scheme 1: Synthesis route of CWPUs-Si

The XPS survey spectra (Fig. 3a) of each sample showed peaks due to carbon (C1s: 285 eV), nitrogen (N1s: 400 eV), and oxygen (O1s: 533 eV). As expected, peaks due to silicon (Si2p: 102 eV and Si2s: 153 eV) were detected in CWPUs-Si3, CWPUs-Si7, and CWPUs-Si11, indicating that the branched SB-PDMS units had been grafted into the CWPUs. Due to the surface enrichment effect, amounts of silicon should represent a mass content gradient from the interior to the exterior of the polymer. To confirm this, XPS survey spectra of a representative sample (CWPUs-Si7) were obtained at different depths (controlled etching time). The high-resolution XPS spectra (C1s) of CWPUs-Si7 in Fig. 3b show that the peak area of C-Si decreased with the detection depth, illustrating that the surface of the film contained more silicon than its interior.

The measured concentrations of silicon (obtained from the XPS survey data; Table 3) revealed that the experimental values were much larger than the theoretical mass contents of each CWPUs-Si film. For example, at 3 wt% CB-PDMS (CWPU-Si3), the measured mass content of silicon (10.85%) was equivalent to an enrichment factor of 9.86, demonstrating efficient accumulation of PDMS units on the surface of the film. Compared with enrichment factors reported for WPUs with PDMS introduced on the polymer backbone,[35] the values obtained from this study were much higher. This confirmed that migration of PDMS located in the side chain of WPU to the polymer/air interface was more efficient than migration from the polymer backbone. The results given in Table 2 also show that the measured silicon content of the CWPUs-Si7 film decreased gradually with increasing detection

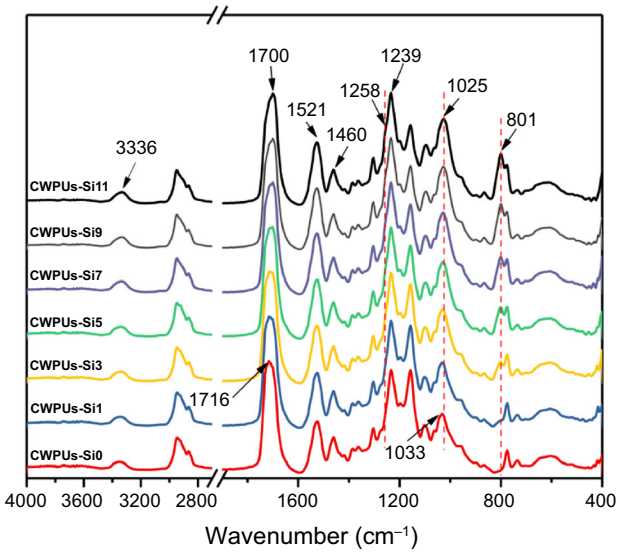

Fig. 1: ATR-FTIR spectra of CWPUs polymer films prepared with increasing contents of SB-PDMS

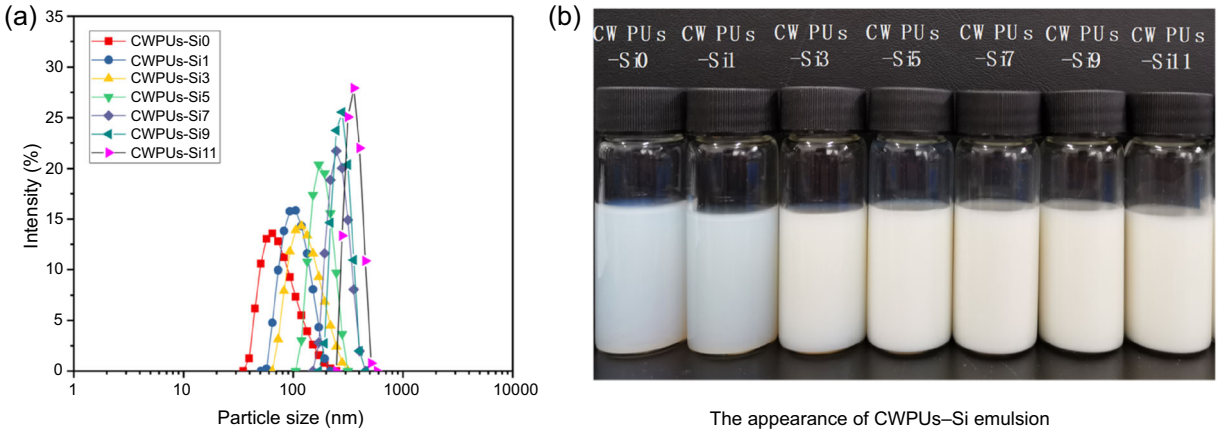

Fig. 2: Particle size distribution (a) and visual appearance (b) of the CWPUs-Si polymers

Table 2: Emulsion properties of CWPUs-Si polymers

Sample	Particle size (nm)	PDI[a]	pH	Viscosity (mPa·s)	Centrifugation sediment	Appearance
CWPUs-Si0	73.6	0.426	3.89	680	No	Translucent
CWPUs-Si1	89.2	0.327	3.84	456	No	Translucent
CWPUs-Si3	120.6	0.179	3.78	100	No	Milky white with blue light
CWPUs-Si5	171.5	0.290	3.78	32	No	Milky white with blue light
CWPUs-Si7	245.6	0.770	3.74	24	No	Milky white with blue light
CWPUs-Si9	271.3	0.951	3.77	20	No	Milky white with blue light
CWPUs-Si11	374.1	1.626	3.77	16	A small amount	Milky white

[a]Refers to particle size polydispersity index

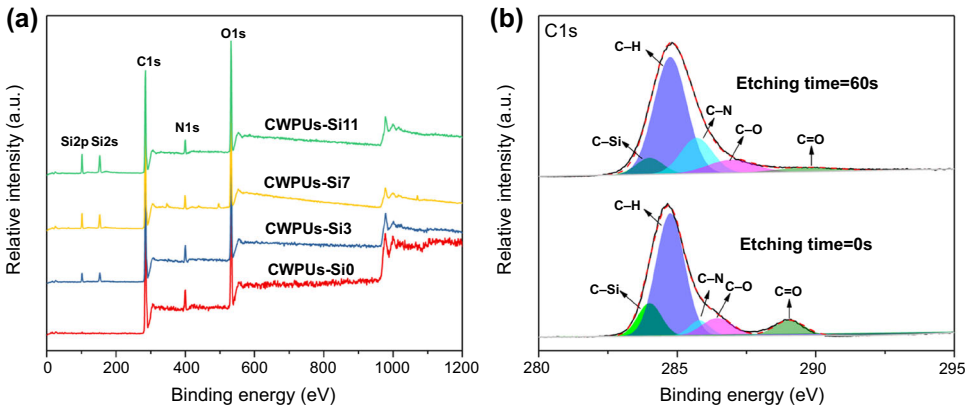

Fig. 3: Surface element investigation of CWPUs-Si films: (a) XPS survey spectra without etching; (b) C1s high-resolution XPS spectra of CWPUs-Si7 film at etching times of 0 and 60 s, respectively

Table 3: Atomic mass contents of CWPUs-Si polymers

Sample	Etching time(s)	Depth (nm)	Mass content (%)					[c]F
			O	N	C	[a]Si	[b]Si	
CWPUs-Si0	0	10.8	26.40	8.98	64.63	0	0	–
CWPUs-Si3	0	10.8	27.13	6.53	55.49	10.85	1.10	9.86
CWPUs-Si7	0	10.8	24.05	4.16	57.54	14.26	2.57	5.55
	30	12.6	15.96	5.65	67.23	11.16	2.57	4.34
	60	14.4	12.72	5.69	72.07	9.52	2.57	3.70
CWPUs-Si11	0	10.8	25.06	4.65	49.93	20.36	4.04	5.09

[a]Measured mass content; [b]Theoretical mass content; [c]Silicon enrichment factor (experimental mass content)/(theoretical mass content)

depth: Without etching (detection depth, 10.8 nm), the silicon mass content was 14.26%; after 60 min etching (detection depth, 14.4 nm), the silicon mass content reduced to 9.52%. Hence, these results provided supporting evidence for a surface enrichment effect in the CWPUs-Si polymer system.

Surface topography of CWPUs-Si

To a large extent, the surface topography mainly depends on the degree of phase separation between the hard segment and soft segment of CWPUs-Si polymers. Figure 4 shows the surface morphology of the CWPUs-Si films obtained using SEM. The surface of the CWPUs-Si0 films revealed micro-scale decorative patterns which reduced in scale following the addition of 3 wt% SB-PDMS (Fig. 4a and 4b). As the content of SB-PDMS increased, the decorative patterns on the surfaces of CWPUs-Si7 and CWPUs-Si11 became more complex (Fig. 4c-d). This increased complexity could arise from increasing phase separation between the hard and soft segments and the decreasing PCL contents. In addition, a more sophisticated surface may contribute to greater surface roughness and surface area of the CWPU-Si films resulting in an increase in the water contact angle of hydrophobic films according to the Wenzel model.[36]

To study the effects of hydrogen bonding on crystal formation, XRD was used to investigate the crystallinity of CWPUs-Si polymers. As shown in Fig. 5, a broad diffraction peak was observed at $2\theta = 19.3°$ for each sample, possibly due to the presence of a microcrystal or the amorphous phase of a soft segment in the CWPUs-Si polymers.[37] Inspection of Fig. 5 shows the intensity of the diffraction peaks decreased with increasing SB-PDMS content, implying that the crystallization of soft segments gradually decreased as the content of PCL (from which they were derived) also decreased. Excessive hydrogen bonding can restrict the movement of soft segments which is detrimental to the formation of a regular structure. The appearance of small diffraction peaks at $2\theta = 12°$ in the spectra of CWPUs-Si7 and CWPUs-Si11 could be attributed to the presence of regular hard segment structures.[38] In addition, the intensity of the diffraction peaks at $2\theta = 12°$ from CWPUs-Si11 was greater than that of CWPUs-Si7. This could be due to the increased polarity of the hard segment resulting from the presence of urea (generated by the amine group in SB-PDMS) and isocyanate groups, which increased the separation between the hard and soft phases to give a more ordered hard segment structure.

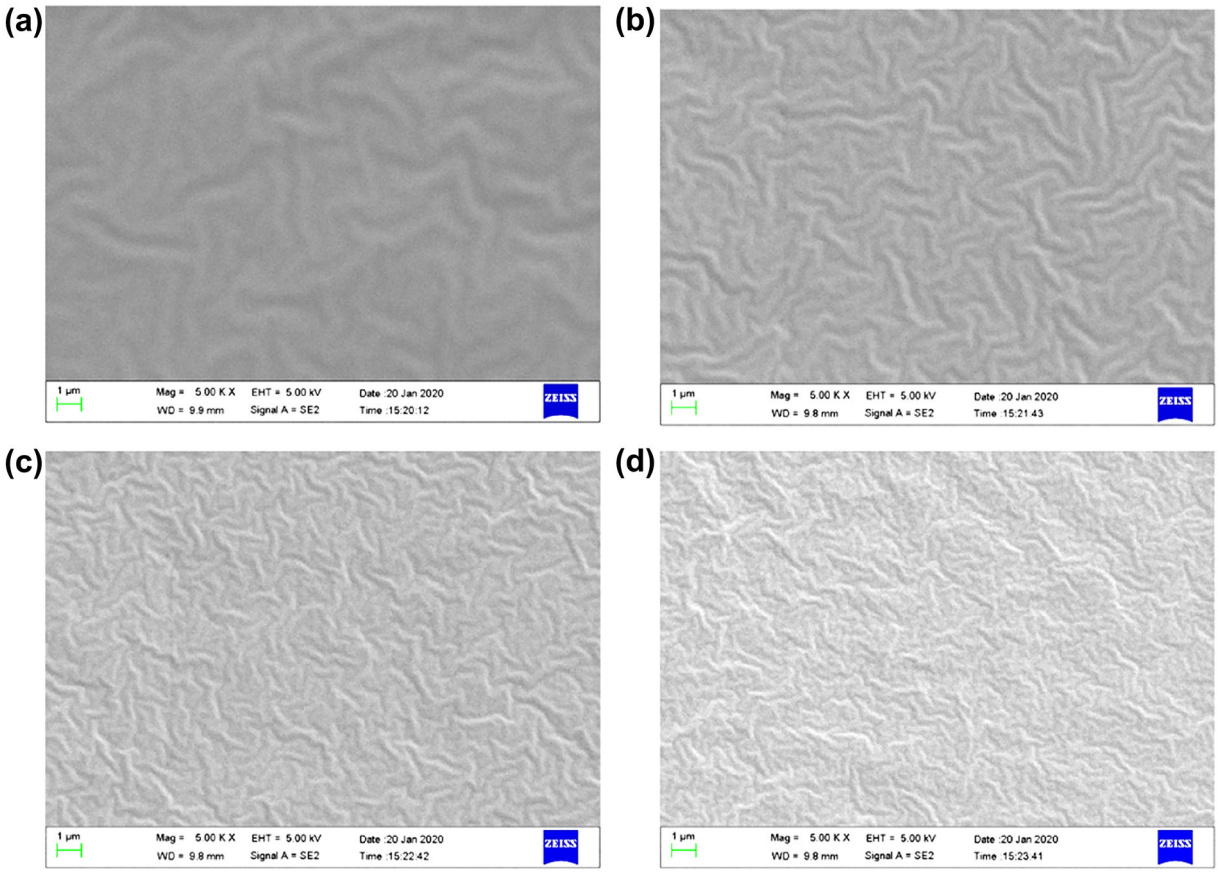

Fig. 4: SEM images showing the surface morphology of CWPUs-Si polymers: (a) CWPUs-Si0; (b) CWPUs-Si3; (c) CWPUs-Si7; and (d) CWPUs-Si11

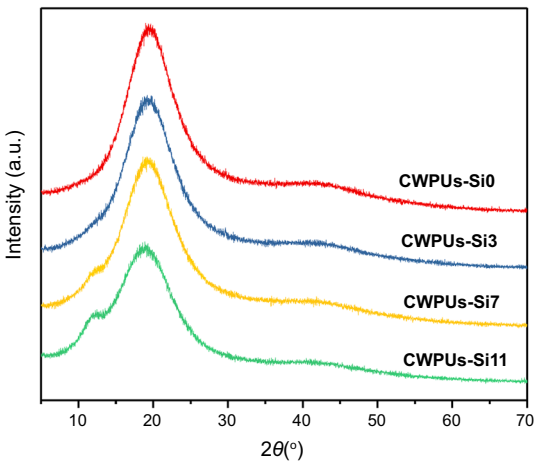

Fig. 5: XRD patterns of CWPUs-Si polymers indicating the effects of hydrogen bonding on crystal formation at each SB-PDMS content level

Water resistance of CWPUs-Si

Water contact angle and water absorption are typically the main indices of water resistance for CWPUs films (Fig. 6a and 6b). The values given for the water contact angle were the average of measurements at five different locations on each sample. Figure 6a shows that the water contact angle of the hydrophilic CWPUs-Si0 film (87.6°) increased rapidly with small additions of SB-PDMS units (1–3%), increasing gradually thereafter to 106.4° at the maximum addition level. These results demonstrated that the surface property of CWPUs-Si0 film could be transformed from hydrophilic to hydrophobic by the introduction of SB-PDMS units with a corresponding improvement in water resistance. The marked increase in water contact angle was due to the incorporation of low surface energy units and the formation of a more sophisticated surface induced by hydrogen bonding.

Figure 6b shows the surface energy, presented as dispersive and polar components, calculated using the water contact angle data. The maximum surface energy of CWPUs-Si0 (dispersive energy = 41.39 mJ m^{-2}; polar component = 1.42 mJ m^{-2}) decreased following the introduction of SB-PDMS to reach a minimum value at 7 wt% addition (mainly the dispersive component; 27.96 mJ m^{-2}), increasing slightly thereafter. The reduction in surface energy could be attributed to the surface enrichment by SB-PDMS and followed the trend in decreasing water absorption, which also attained a minimum value for CWPUs-Si7. Again, it

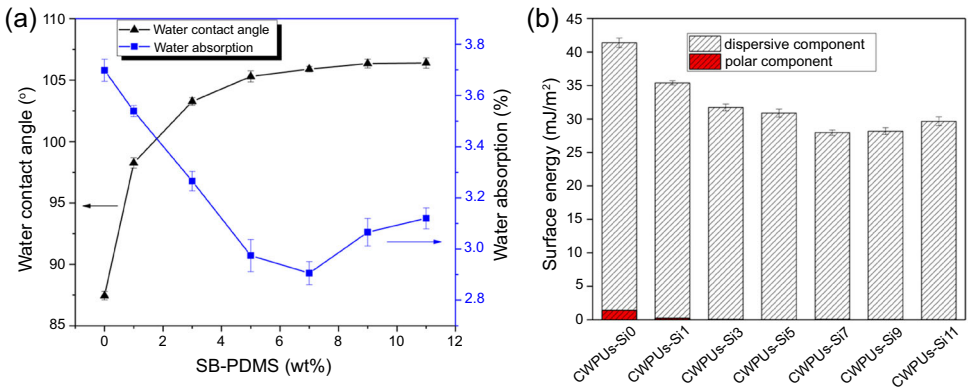

Fig. 6: Effects of SB-PDMS content on the water resistance properties of CWPUs-Si: (a) water contact angle; (b) water absorption; (c) and surface energy

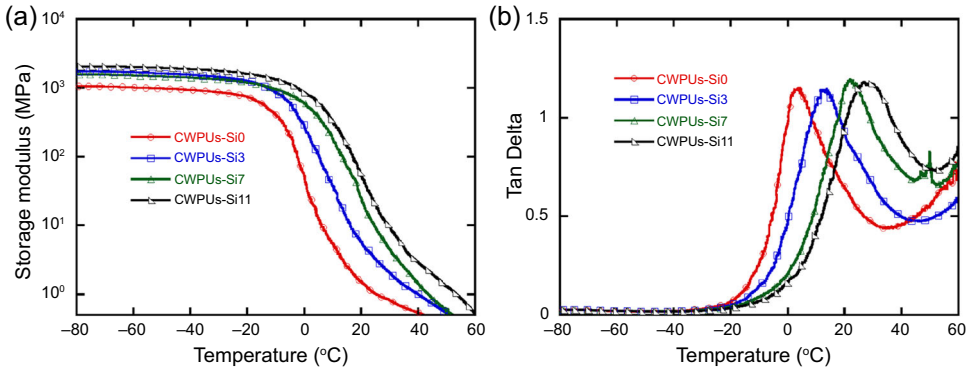

Fig. 7: Effects of temperature on the mechanical properties of the CWPUs-Si polymers: (a) The storage modulus *E'*; and (b) tan δ

could be inferred that the hydrophobic SB-PDMS migrated to the surface of CWPUs-Si film forming a silicone-rich nanoscale layer which improved the water resistance of the CWPUs. The modest increase in the water absorption of CWPUs-Si9/CWPUs-Si11 could be due to disruption of the structural regularity of CWPUs-Si film at the higher levels of CP-PDMS incorporation, thereby permitting some permeation of water within the film.

Mechanical properties of CWPUs-Si

The effects of temperature on the storage modulus (E') and damping (tan δ) response of the CWPUs-Si polymers are shown in Fig. 7.

Figure 7a shows that in the glassy state, the relatively high values of *E'* for each CWPUs film decreased rapidly as the glass transition temperature (T_g) was approached; at 25°C, the *E'* ranged from 1.02 MPa (CWPUs-Si0) to 19.75 MPa (CWPUs-Si11). The peak maxima of tan δ shifted to higher temperature as the amount of SB-PDMS increased, confirming the corresponding increase of T_g; values of T_g ranged from 3.8 to 27.0°C for SB-PDMS incorporation values of 0–11 wt% (Fig. 7b). The increases in *E'* and T_g could be ascribed to the restricted motion of the polymer chains resulting from increased hydrogen bond crosslinking.

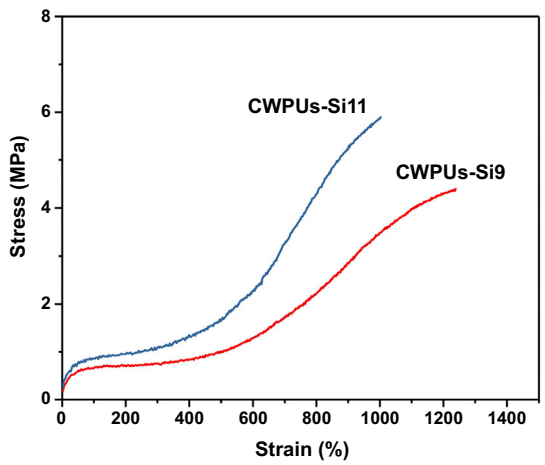

Fig. 8: Stress–strain curves obtained from CWPUs-Si9 and CWPUs-Si11 polymers

At room temperature (25°C), CWPUs with 0–7 wt% CP-PDMS incorporation were in the viscous state (*T* >

Fig. 9: The visual appearance of CED films prepared from the CWPUs-Si polymers

Tg) and their respective stress–strain curves could not be obtained. Hence, Fig. 8 shows the stress–strain curves of CWPUs-Si9 and CWPUs-Si11. The tensile strengths of CWPUs-Si9 and CWPUs-Si11 increased from 4.40 to 5.89 MPa, respectively, while the corresponding elongation at break decreased from 1239 to 1002%.

These observations could be explained by the dependence of hard segments in CWPUs-Si, on the increasing SB-PDMS content (Table 1). Hence, the number of hard segments appeared to enhance the mechanical properties of the CWPUs-Si polymer system. Since physical crosslinking due to hydrogen bonding also limited molecular chain movement, it could be concluded that the improvements in *E'*, Tg, and tensile strength resulted from the increased number of the hard segments and physical crosslinking.

Properties of CED coatings prepared from the CWPUs-Si polymers

The CWPUs-Si polymers were used to prepare CED coatings, and the performance of the resultant films was investigated. Except for the CED film prepared from CWPUs-Si11, the appearance of each CED film was flat and smooth, while the transmittance deteriorated uniformly with increasing SB-PDMS incorporation (Fig. 9). Presumably, the deterioration in transmittance was due to thermodynamic incompatibility between SB-PDMS chains and the CWPU backbone.

The pencil hardness, adhesive force, flexibility, and impact resistance of CED films were measured according to the ISO standards used for paints and varnishes. The pencil hardness of CED films prepared using CWPUs with low SB-PDMS contents (0–7 wt%) were all ranked B, while CWPUs-Si9 and CWPUs-Si11 were ranked HB and H, respectively. The higher pencil hardness scores could be attributed to the increased number of hard segments in the urethane groups. In addition, the results obtained from each polymer for adhesive force (0 grade), flexibility (1 cm), and impact resistance (> 100 kg.cm) indicated optimum performance.

Conclusions

A series of CWPUs-Si polymers were prepared by inserting low surface energy SB-PDMS units into the branched chains of CWPUs. The introduction of SB-PDMS increased the particle size but had no obvious effects on the centrifugal stability of the emulsions. The incorporation of SB-PDMS enhanced phase separation between the soft and hard segment and decreased surface energy due to the surface enrichment with silicon. This increased the water contact angle and decreased water absorption, which greatly improved the water-resistant performance of the polymers. *E'*, T_g and tensile strength also exhibited increases due to the increased number of hard segments and enhanced physical crosslinking. The pencil hardness of CED coatings prepared from each CWPUs polymer increased from B (CWPUs-Si0) to H (CWPUs-Si11), while the SB-PDMS content had no clear effect on their adhesion, flexibility, and impact resistance.

Acknowledgments The study was supported by the Special funds for key areas of ordinary universities in Guangdong Province (Grant No. 2020ZDZX2013), the Basic and Applied Basic Research Major Program of Guangdong Province (Grant No. 2020B1515120001), the Discipline construction project of Guangdong Medical University (4SG21015G,4SG21019G), and the Science and Technology Planning Project of Guangdong Province (Grant No.2017B090915002).

References

1. Nguyen-Tri, P, Tran, HN, Plamondon, CO, Tuduri, L, Vo, D-VN, Nanda, S, Mishra, A, Chao, H-P, Bajp, AK, ''Recent Progress in the Preparation, Properties and Applications of Superhydrophobic Nano-Based Coatings and Surfaces: A Review.'' *Prog. Org. Coat.*, **132** 235–256 (2019)
2. Akindoyo, JO, Beg, MDH, Ghazali, S, Islam, MR, Jeyaratnam, N, Yuvaraj, AR, ''Polyurethane Types, Synthesis and

Applications – A Review.'' *RSC Adv.*, **6** (115) 114453–114482 (2016)
3. Engels, HW, Pirkl, HG, Albers, R, Albach, RW, Krause, J, Hoffmann, A, Casselmann, H, Dormish, J, ''Polyurethanes: Versatile Materials and Sustainable Problem Solvers for Today's Challenges.'' *Angew. Chem. Int. Ed.*, **52** (36) 9422–9441 (2013)
4. Dai, M, Zhai, Y, Zhang, Y, ''A Green Approach to Preparing Hydrophobic, Electrically Conductive Textiles Based on Waterborne Polyurethane for Electromagnetic Interference Shielding with Low Reflectivity.'' *Chem. Eng. J.*, **421** 127749 (2021)
5. Wang, X, Cui, Y, Wang, Y, Ban, T, Zhang, Y, Zhang, J, Zhu, X, ''Preparation and Characteristics of Crosslinked Fluorinated Acrylate Modified Waterborne Polyurethane for Metal Protection Coating.'' *Prog. Org. Coat.*, **158** 106371 (2021)
6. Honarkar, H, ''Waterborne Polyurethanes: A Review.'' *J. Dispersion Sci. Technol.*, **39** (4) 507–516 (2018)
7. Kozakiewicz, J, ''Developments in Aqueous Polyurethane and Polyurethane-Acrylic Dispersion Technology. Part I. Polyurethane Dispersions.'' *Polimery,* 60 (2015)
8. He, X, Zhang, Y, He, J, Liu, F, ''Synthesis and Characterization of Cathodic Electrodeposition Coatings Based on Octadecyl-Modified Cationic Waterborne Polyurethanes.'' *J. Coat. Technol. Res.*, **17** (5) 1255–1268 (2020)
9. Yu, F, Gao, J, Liu, C, Chen, Y, Zhong, G, Hodges, C, Chen, M, Zhang, H, ''Preparation and UV Aging of Nano-SiO_2/Fluorinated Polyacrylate Polyurethane Hydrophobic Composite Coating.'' *Prog. Org. Coat.*, **141** 105556 (2020)
10. Wu, F, Pickett, K, Panchal, A, Liu, M, Lvov, Y, ''Superhydrophobic Polyurethane Foam Coated with Polysiloxane-Modified Clay Nanotubes for Efficient and Recyclable Oil Absorption.'' *ACS Appl. Mater. Interfaces*, **11** (28) 25445–25456 (2019)
11. Liu, X, Zou, X, Ge, Z, Zhang, W, Luo, Y, ''Novel Waterborne Polyurethanes Containing Long-Chain Alkanes: Their Synthesis and Application to Water Repellency.'' *RSC Adv.*, **9** (54) 31357–31369 (2019)
12. Xu, W, Wang, W, Hao, L, Liu, H, Hai, F, Wang, X, ''Synthesis and Properties of Novel Triazine-based Fluorinated Chain Extender Modified Waterborne Polyurethane Hydrophobic Films.'' *Prog. Org. Coat.*, **157** 106282 (2021)
13. Kozakiewicz, J, Ofat, I, Trzaskowska, J, ''Silicone-Containing Aqueous Polymer Dispersions with Hybrid Particle Structure.'' *Adv. Colloid Interface Sci.*, **223** 1–39 (2015)
14. Rahman, MM, Mallik, AK, Khan, MA, ''Influences of Various Surface Pretreatments on the Mechanical and Degradable Properties of Photografted Oil Palm Fibers.'' *J. Appl. Polym. Sci.*, **105** (5) 3077–3086 (2007)
15. Zhang, T, Wu, W, Wang, X, Mu, Y, ''Effect of Average Functionality on Properties of UV-Curable Waterborne Polyurethane-Acrylate.'' *Prog. Org. Coat.*, **68** (3) 201–207 (2010)
16. Sardon, H, Irusta, L, Fernández-Berridi, MJ, Lansalot, M, Bourgeat-Lami, E, ''Synthesis of Room Temperature Self-Curable Waterborne Hybrid Polyurethanes Functionalized with (3-Aminopropyl)Triethoxysilane (APTES).'' *Polymer*, **51** (22) 5051–5057 (2010)
17. Yu, F, Cao, L, Meng, Z, Lin, N, Liu, XY, ''Crosslinked Waterborne Polyurethane with High Waterproof Performance.'' *Polym. Chem.*, **7** (23) 3913–3922 (2016)
18. Zhang, S, RenLiu, Jiang, J, Yang, C, Chen, M and Liu, X, ''Facile Synthesis of Waterborne UV-curable Polyurethane/Silica Nanocomposites and Morphology, Physical Properties of Its Nanostructured Films.'' *Prog. Org. Coat.*, **70** (1) 1-8 (2011)
19. Meng, L, Qiu, H, Wang, D, Feng, B, Di, M, Shi, J, Wei, S, ''Castor-Oil-based Waterborne Acrylate/SiO_2 Hybrid Coatings Prepared via Sol–gel and Thiol-Ene Reactions.'' *Prog. Org. Coat.*, **140** 105492 (2020)
20. Yin, X, Dong, C, Chai, C, Luo, Y, ''Thermostability and Flame Retardance of Green Functional Two-Component Waterborne Polyurethane Coatings with Nanoparticles.'' *Prog. Org. Coat.*, **122** 119–128 (2018)
21. Fu, H, Wang, Y, Chen, W, Xiao, J, ''Reinforcement of Waterborne Polyurethane with Chitosan-Modified Halloysite Nanotubes.'' *Appl. Surf. Sci.*, **346** 372–378 (2015)
22. Zhang, F, Liu, W, Wang, S, Jiang, C, Xie, Y, Yang, M, Shi, H, ''A Novel and Feasible Approach for Polymer Amine Modified Graphene Oxide to Improve Water Resistance, Thermal, and Mechanical Ability of Waterborne Polyurethane.'' *Appl. Surf. Sci.*, **491** 301–312 (2019)
23. He, X, Zhang, X, He, J, Liu, F, ''Preparation and Properties of Hydroxyl-Terminated Cationic Waterborne Polyurethanes for Cathodic Electrodeposition Coatings.'' *Adv. Polym. Tech.*, **37** (8) 3831–3841 (2018)
24. Qiao, X, Chen, R, Zhang, H, Liu, J, Liu, Q, Yu, J, Liu, P, Wang, J, ''Outstanding Cavitation Erosion Resistance of Hydrophobic Polydimethylsiloxane-based Polyurethane Coatings.'' *J. Appl. Polym. Sci.*, **136** (25) 47668 (2019)
25. Zheng, G, Lu, M, Rui, X, ''The Effect of Polyether Functional Polydimethylsiloxane on Surface and Thermal Properties of Waterborne Polyurethane.'' *Appl. Surf. Sci.*, **399** 272–281 (2017)
26. Sharma, S, Mandhani, A, Bose, S, Basu, B, ''Dynamically Crosslinked Polydimethylsiloxane-based Polyurethanes with Contact-Killing Antimicrobial Properties as Implantable Alloplasts for Urological Reconstruction.'' *Acta Biomater.*, **129** 122–137 (2021). https://doi.org/10.1016/j.actbio.2021.04.055
27. Zhang, Z-P, Song, X-F, Cui, L-Y and Qi, Y-H, ''Synthesis of Polydimethylsiloxane-Modified Polyurethane and the Structure and Properties of Its Antifouling Coatings.'' *Coatings*, **8** (5) (2018)
28. Ji, X, Wang, H, Ma, X, Hou, C, Ma, G, ''Progress in Polydimethylsiloxane-Modified Waterborne Polyurethanes.'' *RSC Adv.*, **7** (54) 34086–34095 (2017)
29. Xu, S, Xie, L, Yu, X, Xiong, Y, Tang, H, ''Synthesis and Characterization of Phenyl Polysiloxane Modified Polyurea/Polyurethanes.'' *J. Polym. Sci. Pol. Chem.*, **53** (15) 1794–1805 (2015)
30. Li, Q, Guo, L, Qiu, T, Ye, J, He, L, Li, X, Tuo, X, ''Polyurethane/Polyphenylsilsequiloxane Nanocomposite: From Waterborne Dispersions to Coating Films.'' *Prog. Org. Coat.*, **122** 19–29 (2018)
31. Owens, DK, Wendt, RC, ''Estimation of the Surface Free Energy of Polymers.'' *J. Appl. Polym. Sci.*, **13** (8) 1741–1747 (1969)
32. Król, B, Pielichowska, K, Król, P, Chmielarz, P, ''Polyurethane Cationomers Modified by Polysiloxane.'' *Polym. Adv. Technol.*, **28** (11) 1366–1374 (2017)
33. Du, Y, Zhang, J, Zhou, C, ''Synthesis and Properties of Waterborne Polyurethane-based PTMG and PDMS as Soft Segment.'' *Polym. Bull.*, **73** (1) 293–308 (2016)
34. Hong, C, Zhou, X, Ye, Y, Li, W, ''Synthesis and Characterization of UV-curable Waterborne Polyurethane–Acrylate Modified with Hydroxyl-Terminated Polydimethylsiloxane: UV-cured Film with Excellent Water Resistance.'' *Prog. Org. Coat.*, **156** 106251 (2021)

35. Wu, Z, Wang, H, Tian, X, Cui, P, Ding, X, Ye, X, ''The Effects of Polydimethylsiloxane on Transparent and Hydrophobic Waterborne Polyurethane Coatings Containing Polydimethylsiloxane.'' *Phys. Chem. Chem. Phys.*, **16** (14) 6787–6794 (2014)
36. Mundo, RD, Palumbo, F, Agostino, Rd, ''Nanotexturing of Polystyrene Surface in Fluorocarbon Plasmas: From Sticky to Slippery Superhydrophobicity.'' *Langmuir*, **24** 5044–5051 (2008)
37. Lei, L, Zhang, Y, Ou, C, Xia, Z, Zhong, L, ''Synthesis and Characterization of Waterborne Polyurethanes with Alkoxy Silane Groups in the Side Chains for Potential Application in Waterborne Ink.'' *Prog. Org. Coat.*, **92** 85–94 (2016)
38. Chavan, JG, Rath, SK, Praveen, S, Kalletla, S, Patri, M, ''Hydrogen Bonding and Thermomechanical Properties of Model Polydimethylsiloxane Based Poly(urethane-urea) Copolymers: Effect of Hard Segment Content.'' *Prog. Org. Coat.*, **90** 350–358 (2016)